Pergamon

Int. J. Mach. Tools Manufact. Vol. 35, No. 4, pp. 547–563, 1995

0890-6955/95$9.50 + .00

AN INVESTIGATION OF THE CUTTING FLUID FLOW IN SELF-PILOTING DRILLS

V.P. ASTAKHOV,†‡ P. S. SUBRAMANYA† and M. O. M. OSMAN†

(*Received* 28 *October* 1993; *in final form* 8 *April* 1994)

Abstract—The conditions of the coolant flow through the inlet annular channels, machining zone and outlet channels of self-piloting drills were investigated. Experiments were performed on B.T.A. and Ejector drills to determine the influence of the drill design parameters on the flow parameters. The influence of the inlet channel's clearance and eccentricity on the pressure distribution and energy loss was analytically examined. Experimental investigations of the static and dynamic pressure distribution of the cutting fluid in the machining zone were performed with different drill heads. Conditions for reliable chip removal from the machining zone and the boring bar were defined. The results obtained constitute a reference for designers of self-piloting drills and drilling processes.

1. INTRODUCTION

DEEP hole machining with self-piloting drills has come a long way since its inception by the Boring and Trepanning Association (B.T.A.). Even though a substantial amount of research has been done in this field, a lot more remains to be done to establish an analytical design methodology for the efficient design of self-piloting tools. There are several types of self-piloting deep hole drills used in industry. This paper deals with the B.T.A. and Ejector drills.

Figure 1 shows the principle of the B.T.A. drilling process. The B.T.A. tool consists of a boring bar, a single or a multi-edged drill head, and a pressure head. The cutting fluid is pumped through the inlet in the pressure head and flows through the annular channel between the boring bar and the bore wall toward the drill head. After cooling and lubricating the machining zone, the cutting fluid carries away the chips through the interior of the drill head and the boring bar. Under optimal drilling conditions, the returning chips do not come into contact with the bore wall thus an excellent bore finish is obtained.

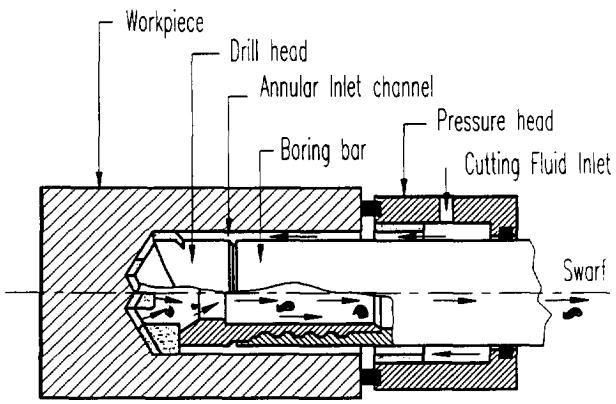

FIG. 1. Principle of the B.T.A. deep hole drilling process.

†Department of Mechanical Engineering, Concordia University, Montreal, Quebec, Canada H3G 1M8.
‡Visiting scholar from Department of Machine Tool Engineering, Odessa Polytechnic University, Ukraine 270044.

Figure 2 shows the principle of the Ejector drilling process. The Ejector drilling system comprises a connector, an outer tube (boring bar), an inner tube and a multi-edged drill head. The cutting fluid is pumped into the machining zone through the inlet in the connector and flows through the annular channel between the boring bar and the inner tube. Most of the cutting fluid is forced through the holes in the drill head for cooling and lubricating the cutting edges and the supporting pads. The remaining part is diverted directly back through the inner tube via ejector nozzles. This diversion produces the ejector effect, i.e. it creates a partial vacuum in the inner tube. This induced vacuum promotes the flow of the cutting fluid along with the chips from the machining zone toward the outlet through the inner tube.

The effectiveness of the self-piloting drills depends to a large extent on the pressure loss and pressure distribution of the cutting fluid along the hydraulic circuit of the drills [1–4]. This circuit, for the B.T.A. and Ejector drills, could be divided into three zones: inlet annular channel, machining zone and chip removal channel. This paper presents the results of a theoretical and experimental investigation of cutting fluid flow in the hydraulic circuit of the B.T.A. and Ejector drills. The study was conducted in order to understand the influence of the drill design parameters of the cutting fluid flow.

2. PRESSURE DISTRIBUTION AND LOSS ALONG THE ANNULAR INLET CHANNELS

In B.T.A. drilling and particularly in Ejector drilling, the annular channels are narrow so that high rigidity of the boring bar is attained while allowing for maximum cross-sectional area of the internal chip removal channel. Therefore, the Navier–Stokes equations can be represented by only one equation for the axial velocity, v_z, of the cutting fluid [5]. The other velocity components are assumed to be insignificant or zero, i.e.

$$\frac{\partial^2 v_z}{\partial r^2} + \frac{1}{r}\frac{\partial v_z}{\partial r} = \frac{1}{\mu_c}\frac{dp}{dz} \tag{1}$$

with the following boundary conditions

$$r = R_1 \qquad v_z = 0$$
$$r = R_2 \qquad v_z = 0\,. \tag{2}$$

Solving equation (1) subject to the boundary conditions (2), along with the continuity flow equation, the following integral equation (in non-dimensional coordinates) for pressure distribution along the annular channel is obtained:

$$p = -12\mu_c L C_1 \int \frac{dz}{R_1 \delta_0^3} \pm 6\mu_c L \int \frac{dz}{\delta_0^2} + C_2\,. \tag{3}$$

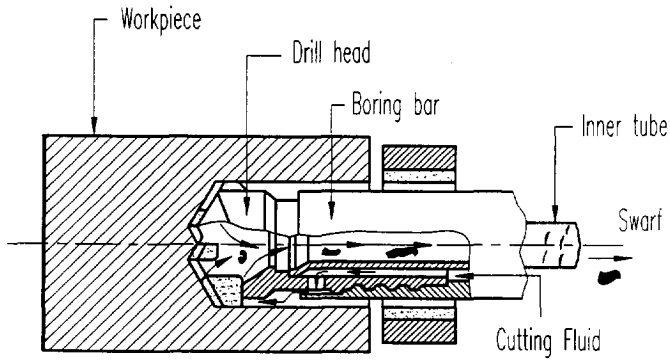

FIG. 2. Principle of the Ejector deep hole drilling process.

Here, $\delta_0 = R_2 - R_1$; where R_2 and R_1 are the radii of the external and internal channel walls, respectively, L is the length of the annular channel, μ_c is the dynamic viscosity of the cutting fluid, and C_1 and C_2 are constants. The "±" signifies the axial movement of one of the annular channel walls, "+" corresponds to coinciding flow and wall velocity, while, "−" corresponds to opposing flow and wall velocities.

In reality, the inlet channels in deep hole drills, especially in Ejector drills, are eccentric and their sizes also vary along the length of the boring bar. If ε is the eccentricity of the annular channel (Fig. 3), then the relative eccentricity is

$$\bar{\varepsilon} = \frac{\varepsilon}{\delta_0} . \tag{4}$$

If $\varepsilon = 0$ then $\bar{\varepsilon} = 0$; this case corresponds to the nominal location of the annular channel's walls. If $\varepsilon = \delta_0$ then $\varepsilon = 1$; this case corresponds to contact between the annular channel's walls. Thus, the variable clearance between the channel's walls is

$$\delta(z,\varepsilon,\theta) = (R_2 - R_1) - \varepsilon\cos\theta + (R_2 - R_1)\frac{z}{L} , \tag{5}$$

or in non-dimensional coordinates

$$\delta(z,\bar{\varepsilon},\theta) = \delta_0(1 - \bar{\varepsilon}\cos\theta + k\bar{z}) , \tag{6}$$

where k is

$$k = \frac{\delta_{02} - \delta_{01}}{\delta_{01}} \quad \text{and}$$

$$\bar{z} = \frac{z}{L} . \tag{7}$$

Here, δ_{01} and δ_{02} are the clearances in the inlet and outlet sections of the annular channel, respectively.

Therefore, the equations of the channel walls are

$$R_1 = R_2 \tag{8}$$

and

$$R_2(z,\bar{\varepsilon},\theta) = \delta_0(z,\bar{\varepsilon},\theta) + R_1 . \tag{9}$$

Integrating (3) subject to the boundary conditions of equations (6), (8) and (9), yields

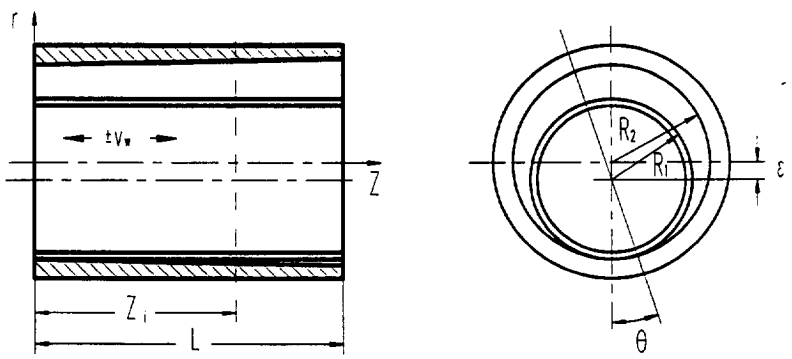

FIG. 3. Diagram of the annular channel.

$$p = \frac{6\mu_c L C_1}{R_1 \delta_{01}^3 k(C + k\bar{z})^2} \pm \frac{6\mu_c L v_w}{\delta_{01} k(C + k\bar{z})} + C_2, \tag{10}$$

where $C = 1 - \varepsilon\cos\theta$ and v_w is the axial velocity of the wall.

The following boundary conditions were used to obtain C_1 and C_2,

$$\text{for,} \quad \bar{z} = 0\,, \quad p = p_{in0} \quad \text{and}$$
$$\text{for,} \quad \bar{z} = 1\,, \quad p = p_1\,. \tag{11}$$

Here, p_{in0} and p_1 are the cutting fluid pressure at the inlet and outlet sections of the annular channel, respectively.

Then equation (10) becomes

$$p = p_{in0} - \frac{(C - k)(2C\bar{z} + k\bar{z}^2)}{(2C + k)(C + k\bar{z})^2} \pm A \frac{k\bar{z}(\bar{z} - 1)}{(2C + k)(C + k\bar{z})^2}\,, \tag{12}$$

where

$$A = \frac{6\mu_c v_w L}{\delta_{01}^2 \Delta p}\,. \tag{13}$$

Here Δp is the pressure difference between the inlet and outlet sections of the annular channel for stationary walls.

2.1. *Particular cases of cutting fluid flow*

(1) The annular channel walls are stationary cylinders with parallel axes ($k = 0$). Then from equation (12) the following expression for non-dimensional pressure is obtained

$$p(\bar{z}) = p_{in0} - \bar{z}\,. \tag{14}$$

It is evident from equation (14) that the non-dimensional cutting fluid pressure varies linearly along the channel's length regardless of eccentricity.

(2) If the walls of the channel are relatively stationary ($v_w = 0$) then $k \neq 0$. In the particular case of concentric walls ($C = 1$) equation (12) becomes,

$$p(\bar{z},k) = p_{in0} - \frac{(1 - k)^2(2\bar{z} + k\bar{z}^2)}{(2 + k)(1 - k\bar{z})^2}\,. \tag{15}$$

It can be seen from Fig. 4 that the pressure drop increases significantly with increasing k. For the case of the eccentric walls ($\varepsilon \neq 0$),

$$p = p_{in0} - \frac{(C + k)^2(2C\bar{z} + k\bar{z}^2)}{(2C + k)(C + k\bar{z})^2}\,. \tag{16}$$

The pressure loss along annular channels can be defined by using the friction factor for annular channels, f_{ag} (Fig. 5), as follows

$$\Delta p = \gamma_{cf} \cdot h_L\,, \tag{17}$$

where, γ_{cf} is the specific gravity of the cutting fluid and h_L is the head loss along the channel given by,

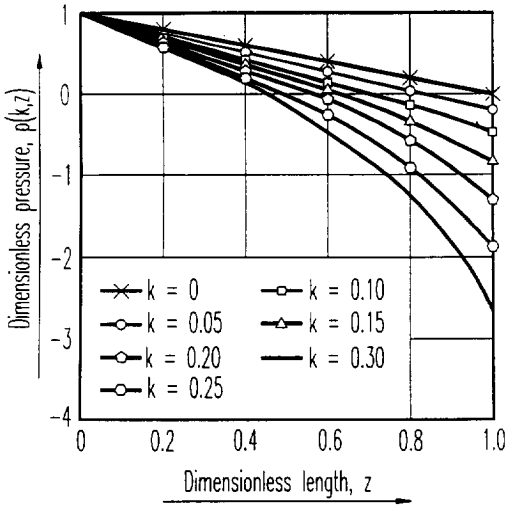

FIG. 4. Pressure distribution along the annular channel.

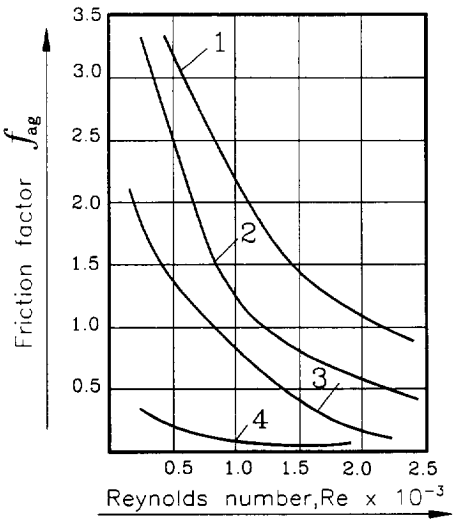

FIG. 5. Friction factor vs Reynolds number: (1) pure oil; $\nu_{50} = 0.17 \times 10^{-4}$; (2) oil-based cutting fluid "MR3"; $\nu_{50} = 0.17 \times 10^{-4}$; (3) oil-based cutting fluid "SHELL GARIA H" and (4) water-based fluid.

$$h_L = f_{ag} \frac{L}{R_e} \frac{v_z^2}{4g}, \tag{18}$$

where the equivalent radius of the annular channel R_e is given by,

$$R_e = \sqrt{(R_2^2 - R_1^2)}, \tag{19}$$

where R_2 and R_1 are the external and internal radii of the channel walls.

While drilling, at least one of the channel walls is rotating. Three commonly used kinematic schemes of B.T.A. drilling are:

(1) Rotating Workpiece–Stationary Tool. In this case the outer wall of the inlet annular channel is rotating.

(2) Stationary Workpiece–Rotating Tool. In this case the inner wall of the channel is rotating.

(3) Counter-Rotation. In this case both walls of the channel are rotating but in opposite directions.

The experimental results show that the hydraulic resistance of the inlet annular channels increases directly with increasing rotational velocity of the channel walls. The following experimental formula defines the friction factor, f_R, for the rotational velocity v_b of the boring bar

$$f_R = f_{ag}\left[1 + 0.5\left(\frac{v_b}{v_z}\right)^2\right]^{0.535}. \tag{20}$$

3. CUTTING FLUID FLOW IN THE MACHINING ZONE

The special geometry of the drill head results in the formation of a special bottom of the hole during drilling (Fig. 6). The space enclosed by bottom from one side and the flanks of the drill head from other is called the "bottom clearance". The cutting fluid pressure in the bottom clearance has a major influence on the cooling and lubricating conditions of the flank and rake contact areas. Increasing the cutting fluid pressure in the bottom clearance provides better penetration of the oil-based cutting fluid to the narrow passages between the tool flanks and the bottom, i.e. better conditions for lubrication and cooling of the flank contact areas. Therefore the pressure in the regions close to the cutting edge(s) should be as high as possible under a given flow rate. This leads to a considerable reduction in flank wear and therefore increases the tool life [6]. Unfortunately little has been known about the effect of the drill design parameters on the cutting fluid pressure distribution in the bottom clearance.

Several experiments were performed to investigate the influence of the drill head design on the cutting fluid pressure distribution in the bottom clearance using a single edge B.T.A. solid boring head (Drill "A" American Heller) and a multi-edge VKW solid drilling head (Drill "B"). The diameter of each drill was 50.8 mm (2"). Some design parameters of the drill heads are shown in Figs 7 and 8.

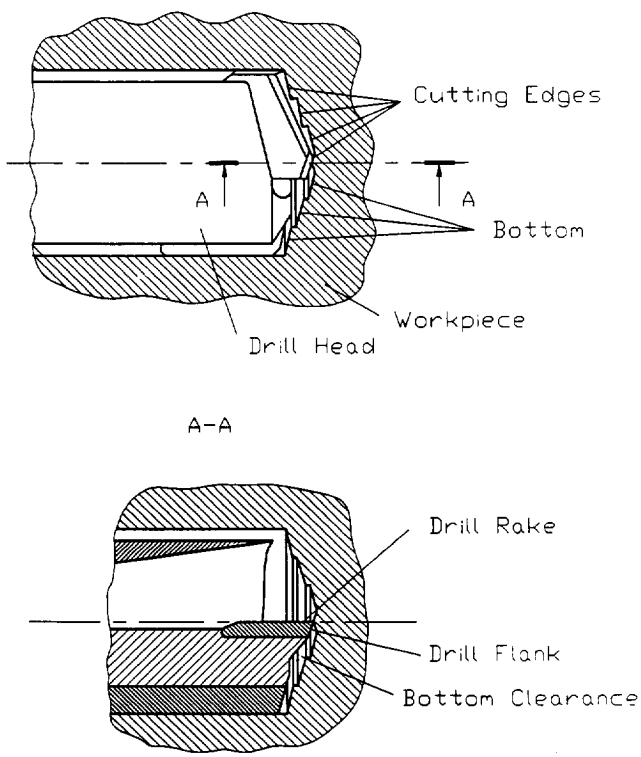

FIG. 6. Drill head forming the bottom clearance.

Figure 9 shows the drilling machine installation used in the experiments. The installation consisted of a drive unit, a pressure head, a boring bar and drill head, chip traps and filters, precise turbine flow meter and a high pressure cutting fluid flow station. The station was capable of delivering a flow of up to 220 l/min and generating a pressure of 4.5 MPa. The precision turbine flow meter (accuracy ±1%) was used to measure the flow rate that was controlled by a flow rate regulator. The stationary workpiece–rotating tool working method was used in the experiments. The setups required for both the static and dynamic pressure acquisition experiments (referred to in "Detail A" of Fig. 9) are shown in Figs 10 and 11, respectively, which show the parts involved (refer to Fig. 9). The workpiece was a cylindrical Plexiglas bar (diameter 75 mm) pre-drilled by the test drill into a blind hole. The blind end was provided with many 8 mm diameter bleed holes to coincide with the cutting edges of the drill heads. The bleed holes of the workpiece are tapped and fitted with barbed screws to allow poly-tubes to be connected to the screws. The workpiece was then held tightly inside the chuck such that the poly-tubes were still accessible and the bleed holes were horizontally aligned. The drill head was attached to the boring bar. The pressure head was advanced towards the workpiece and was hydraulically pressed onto it. The boring bar was advanced until the cutting tool touched the bottom of the workpiece.

The auxiliary parts needed for the static pressure distribution measurements are shown in Fig. 10. Pressure gauges (ranging from 0 to 600 kPa), bleed screws, a pointer

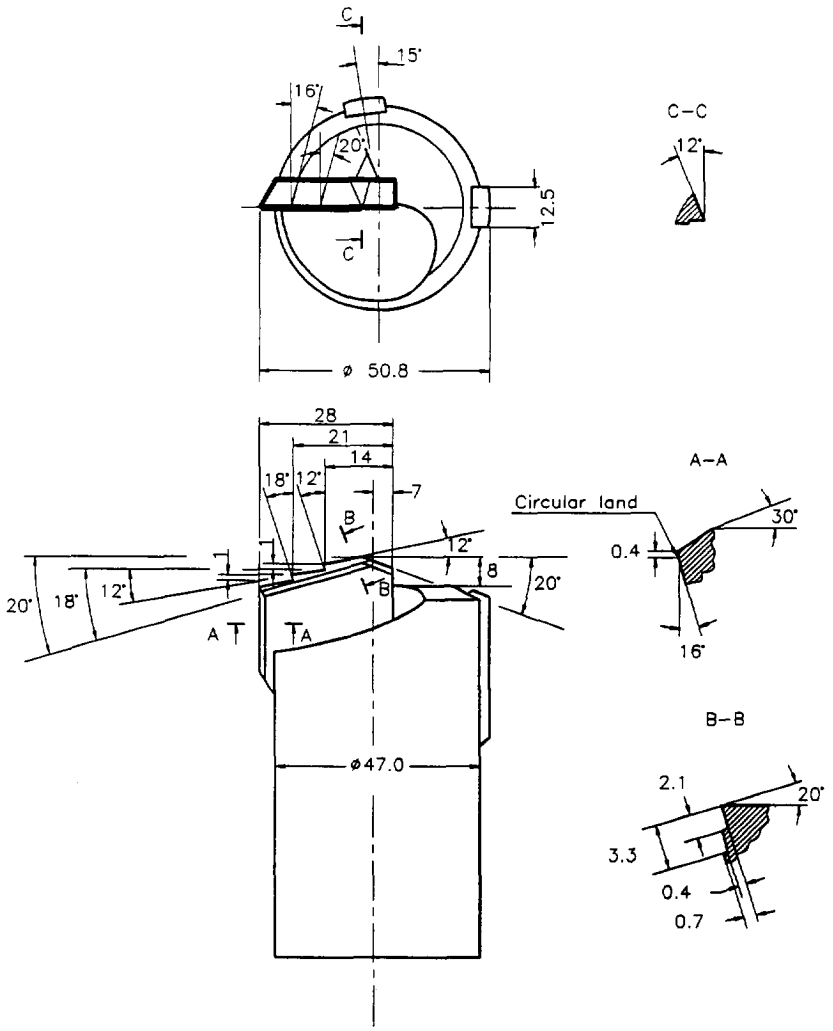

FIG. 7. Design parameters of a single edge B.T.A. solid boring head (Drill "A").

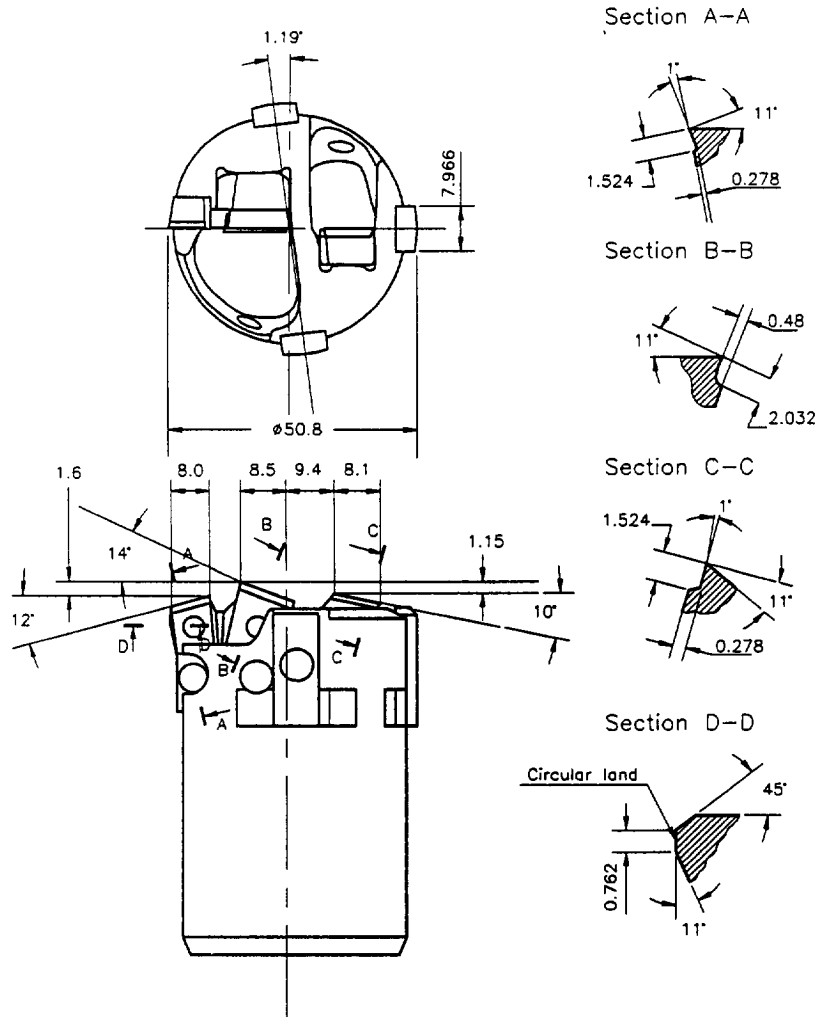

FIG. 8. Design parameters of a multi-edge B.T.A. solid boring head (Drill "B").

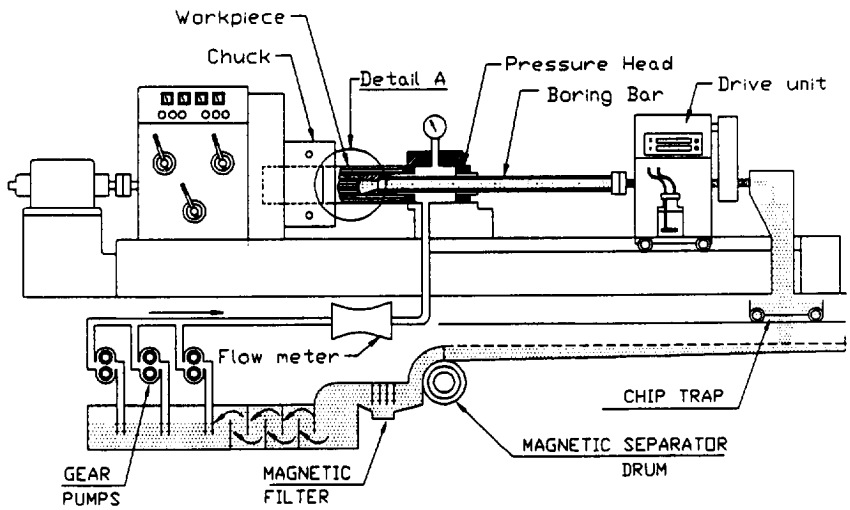

FIG. 9. Drilling machine's installation used in the experiments.

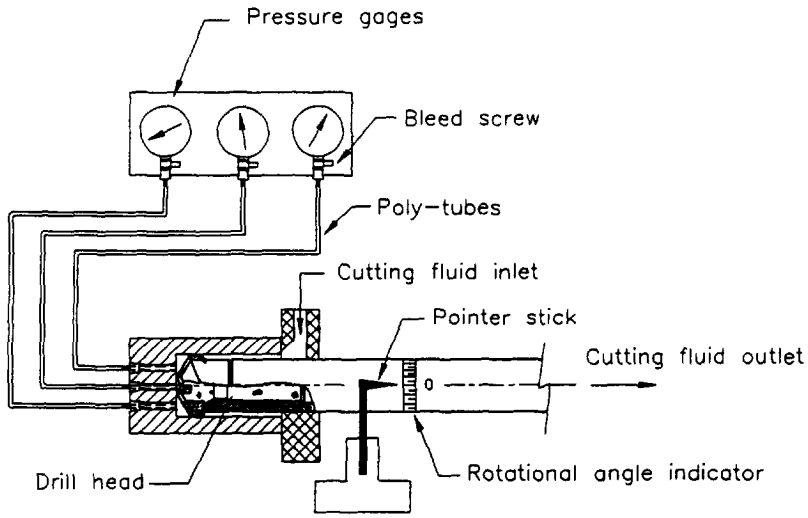

FIG. 10. Setup for static pressure acquisition experiment.

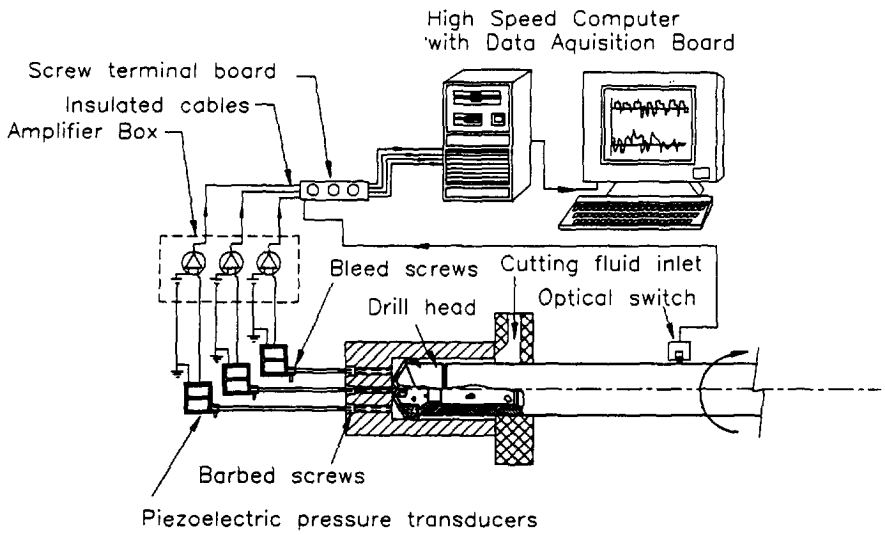

FIG. 11. Setup for dynamic pressure acquisition experiment.

stick and a rotational angle indicator on the boring bar were the main components of the setup.

The boring bar was rotated until the edge of the cutting tool was collinear with the drilled through-holes, and the rotational angle indicator was set to zero relative to the pointer. The pressure gauges were attached to the bleed screws which in turn were connected to the poly-tubes. Later the lubricant flow was set to ON, and the trapped air was removed from the poly-tubes with the aid of the bleed screws. Finally the pressure was read for different angular positions of the boring bar for a complete cycle. This procedure was repeated for several flow rates varying from 115 to 170 l/min. The results were plotted on cycle graphs and examples are shown in Fig. 12.

The dynamic pressure distribution measurements were recorded using (refer to Fig. 11) a computer controlled data acquisition system (OMEGA:DAS-20), screw terminal board, piezoelectric pressure transducers (DP15TL) with the corresponding amplifier box, an optical switch (OPB-804) and insulated cables.

The pressure transducers are connected to the bleed holes on the workpiece using poly-tubes and bleed screws. The signals from the pressure transducers were amplified and sent to the data acquisition system. The optical switch mounted close to the boring

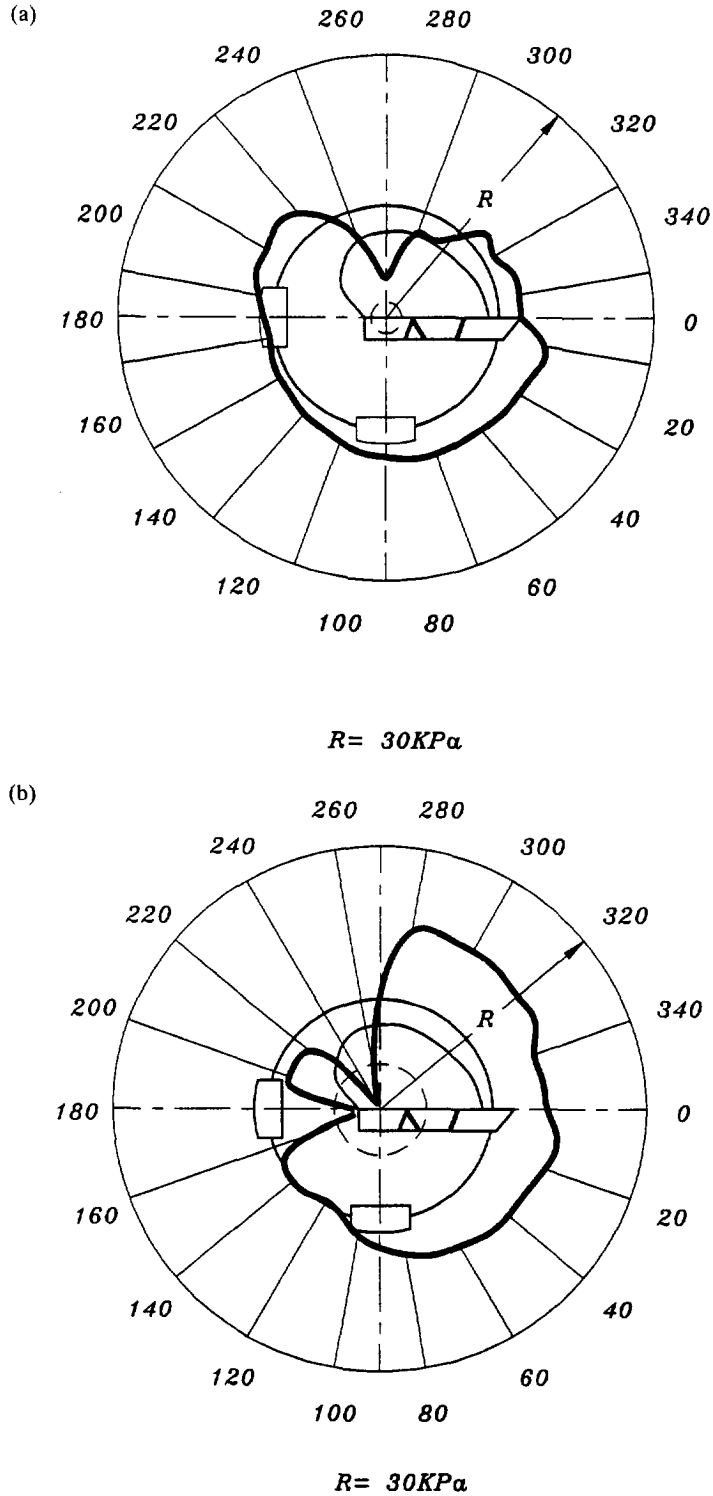

FIG. 12. Examples of the static pressure distribution in the bottom clearance: (a) drill "A", position of the transducer hole corresponds to r = 3.1 mm; (b) drill "A", position of the transducer hole corresponds to r = 10.6 mm; (c) drill "B", position of the transducer hole corresponds to r = 6.5 mm and (d) drill "B", position of the transducer hole corresponds to r = 15.5 mm.

(c)

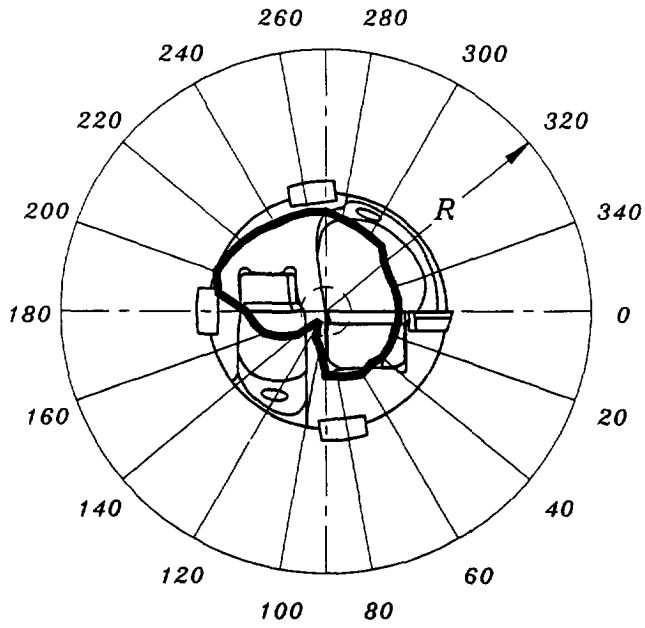

R=250 KPα

(d)

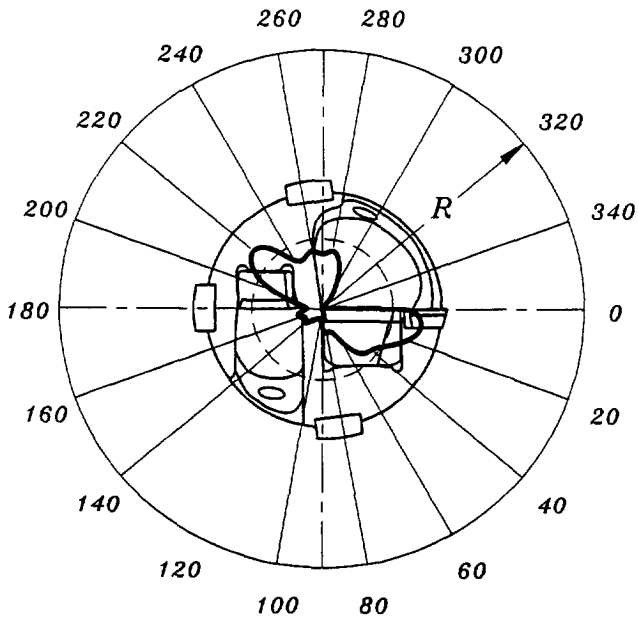

R= 250KPα

FIG. 12. Continued.

bar is connected to the data acquisition system in the computer through an amplifier. The purpose of this switch is to signal the beginning and the end of a complete cycle of the boring bar rotation. The flow was set ON, the trapped air in the poly-tubes was removed, the system was allowed to reach steady state conditions and the data acquisition procedure was started. The data were collected at a rate of 5000 samples/s. The data was later analyzed and plotted on cycle graphs and examples are shown in Fig. 13.

Analysis of the experimental results shows that:

(1) The static as well as the dynamic pressure distribution in the machining zone were not uniform, contrary to the currently held view. Both distributions change significantly in the bottom clearance and there exist regions with zero pressure or negative pressure in the machining zone under static and dynamic conditions.

(2) The rotation of the tool leads to a significant change in the pressure distribution in the bottom clearance (refer to Figs 12(a)–(d) and Figs 13(a)–(d)). The rotation makes the distribution more uniform in the case of drill "A" and less uniform in the case of drill "B". This seems to be due to the swirling effect produced by the drill head features as in the case of drill "B".

(3) In deep hole drilling, the tool life is defined by the flank wear of the cutting edge(s). It is known that flank wear is influenced by the rate of penetration of the cutting fluid to the contact areas between the bottom of the hole and the flank(s). This rate depends upon both the properties of the cutting fluid and its static pressure in the region adjacent to the flank contact areas. The results (Figs 12 and 13) show that drill "B" has a higher cutting fluid pressure in these areas. For drill "A", the zone of maximum pressure is shifted to the direction of the second supporting pad and plays no role in improving the cooling and lubrication of the cutting edge.

(4) The architecture of drill "A" provided better conditions for the chip removal process due to a more uniform pressure distribution at the mouth of the chip removal tube. In the case of drill "B", sufficient conditions were achieved in the regions adjacent to the rake surface, but near the chip mouth, the pressure was high. This can be explained by the presence of the additional screw holes in the drill head, which were sources of additional cutting fluid jets directed toward the chip mouth. The existence of these jets can hinder the chip removal process through the chip mouth and along the throat, which are the most critical passages of the chip removal system.

(5) The results also showed that the architecture of the drill head can be changed to achieve a better pressure distribution, avoid negative pressure regions in the bottom clearance, and provide better conditions for cooling, lubrication and the chip removal.

4. CHIP REMOVING ALONG THE INTERNAL CHANNELS

Reliable chip removal is one of the most important requirements of deep hole drilling. As mentioned above, after performing its cooling and lubricating actions in the machining zone, the cutting fluid carries away the chips through the interior of the drill head and the boring bar. Therefore after the machining zone, a two-phase flow medium exists along the internal channels. The most important factors affecting this two-phase flow medium are;

(i) the density and viscosity of the cutting fluid as a function of its temperature;

(ii) the chip concentration (weight or volumetric), rheological properties and velocity of the cutting fluid–chip mixture and

(iii) the cross-sectional area and profile configuration of the chip removal channels.

The flow of the cutting fluid chip mixture through the chip removal channel may occur in different transportation modes; heterogeneous with a gliding chip layer, heterogeneous, and pseudohomogeneous. Figure 14 illustrates the velocity and concentration profiles, and the relationship between the mixture velocity and the friction loss along the chip removal channel for each mode.

The mixture velocity corresponding to the beginning of the heterogeneous mode is termed the "critical velocity" (v_{cr}). Observations showed that if the mixture's velocity was less than v_{cr}, the formed chips would accumulate in the boring bar thus blocking

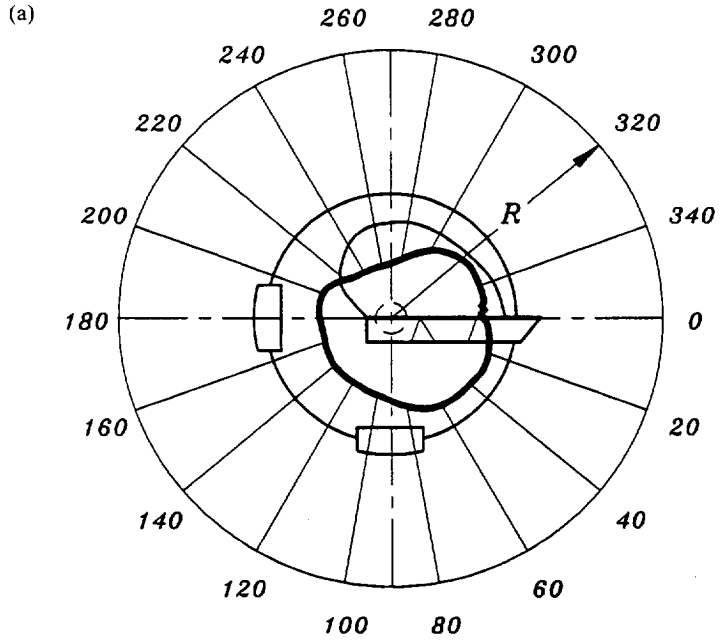

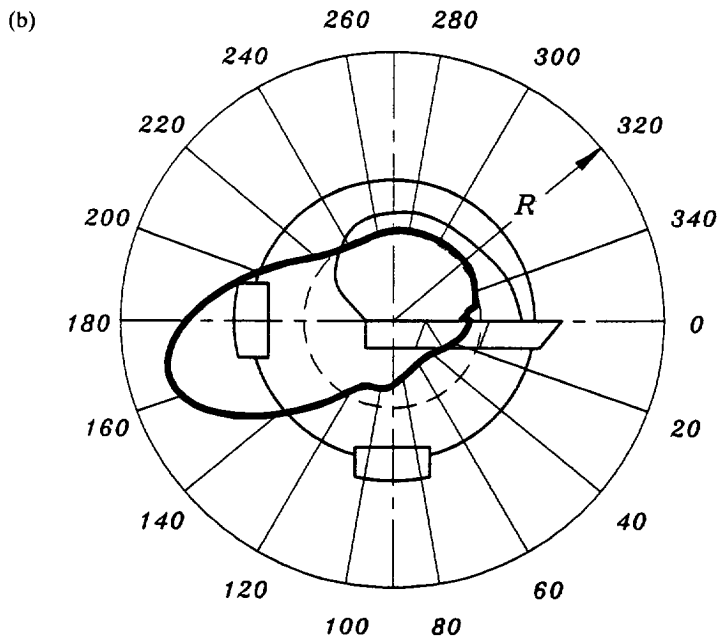

FIG. 13. Examples of the dynamic pressure distribution in the bottom clearance: (a) drill "A", position of the transducer hole corresponds to r = 3.1 mm; (b) drill "A", position of the transducer hole corresponds to r = 13.1 mm; (c) drill "B", position of the transducer hole corresponds to r = 3.1 mm and (d) drill "B", position of the transducer hole corresponds to r = 13.1 mm.

(c)

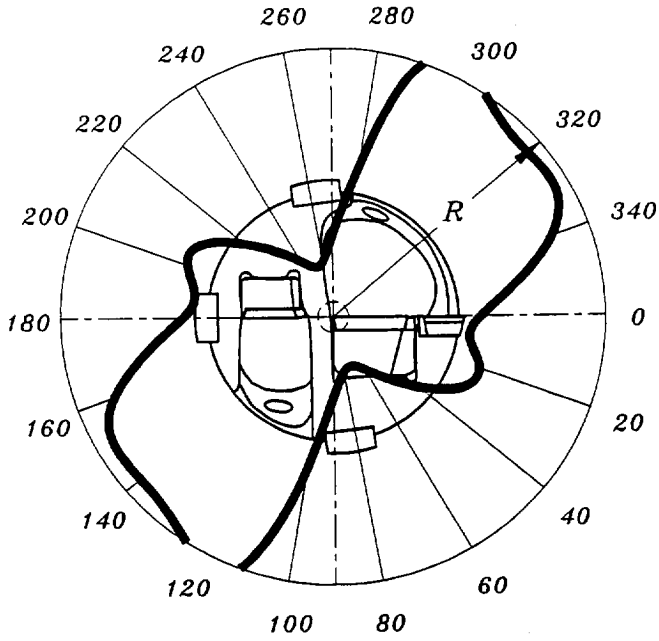

$R = 500KP\alpha$

(d)

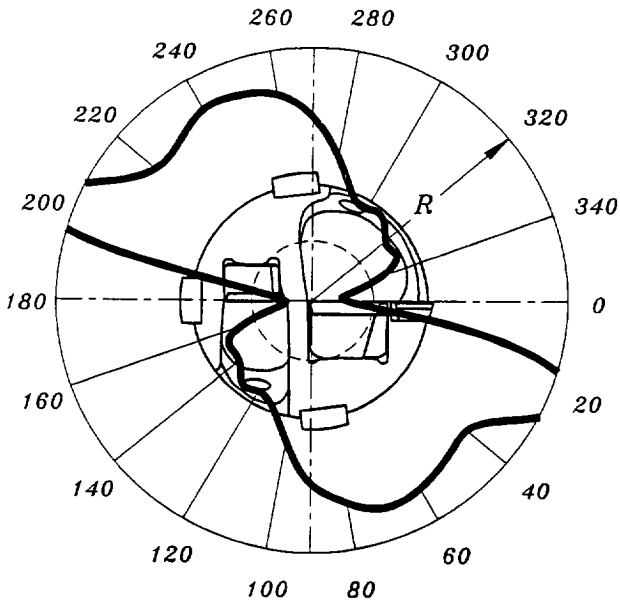

$R = 500KP\alpha$

FIG. 13. Continued.

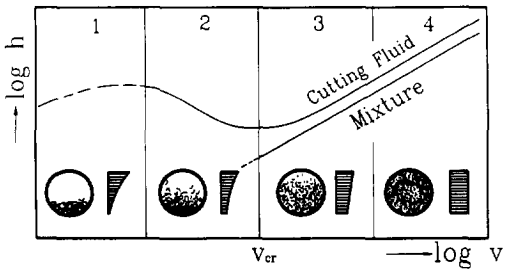

FIG. 14. Friction loss along the chip removal channel for different flow modes of the cutting fluid–chip mixture: (1) flow break with the stationary layer; (2) heterogeneous flow with the gliding layer; (3) heterogeneous and (4) pseudohomogeneous.

the chip removal process. As a result, the drilling process had to be stopped. Reliable chip removal can be achieved when the mixture velocity at any cross-section of the chip removal channels is greater than the critical velocity.

The critical velocity of the mixture can be defined from the analysis of the three main components of the total mixture head loss, h_m,

$$h_m = h_L + h_I + h_F \,, \tag{21}$$

where h_L is the friction loss of the chip removal channels, h_I is the loss due to the cutting fluid–chip interaction under transportation, and h_F is the loss from the energy necessary to maintain the chips in the flow conditions.

From the experimental results and similarity theory applied to the pressure loss in the mixture flow, the following empirical formula for the critical velocity of the cutting fluid–chip mixture has been established [7],

$$v_{cr} = 8.44\left[C_w\left(\frac{\gamma_m}{\gamma_{cf}} - 1\right) g\, v_c\, A_c^{1/2}\right]^{1/3} . \tag{22}$$

Here, C_w is the weight concentration of the chip in the mixture, γ_m is the specific gravity of the chip material, g is the gravitation constant, v_c is the free-fall velocity of the chip in the stable cutting fluid and A_c is the cross-sectional area of the chip removal channel.

The tests which were carried out to establish the conditions for reliable chip removal along the internal passage of the B.T.A. and Ejector drills provided a reasonable velocity. A reasonable velocity of the mixture, which implies a reasonable flow rate, is recommended to be 15 to 21 percent higher than the critical velocity, i.e.

$$v_{res} = (1.15 \text{ to } 21)\, v_{cr}. \tag{23}$$

To achieve reliable chip removal, the velocity greater than the reasonable velocity should be provided at all cross-sections of the passage in the chip removal system.

In certain cases it was not possible to provide v_{res} for each passage in the whole chip removal system of the drilling machine. It was common for small diameter drills (6–30 mm), and in the case of necessity, to transport the mixture far away from the machine receiver. An additional flow of cutting fluid was introduced behind the tool–workpiece interface. In these cases, the total flow rate for the chip removal system was determined that v_{res} (Q_0) was secured at any downstream section of this system (Fig. 15 shows such application). The additional flow of cutting fluid Q_1 was fed through the fitting 1 to the operating chamber 2. This flow passed through the ejector nozzle 3 to the mixing chamber 4. Due to this flow a lower pressure region was created in chamber 5, promoting the flow of cutting fluid with the chips along the boring bar. In the mixing chamber 4 the resulting cutting fluid–chip mixture velocity exceeded the

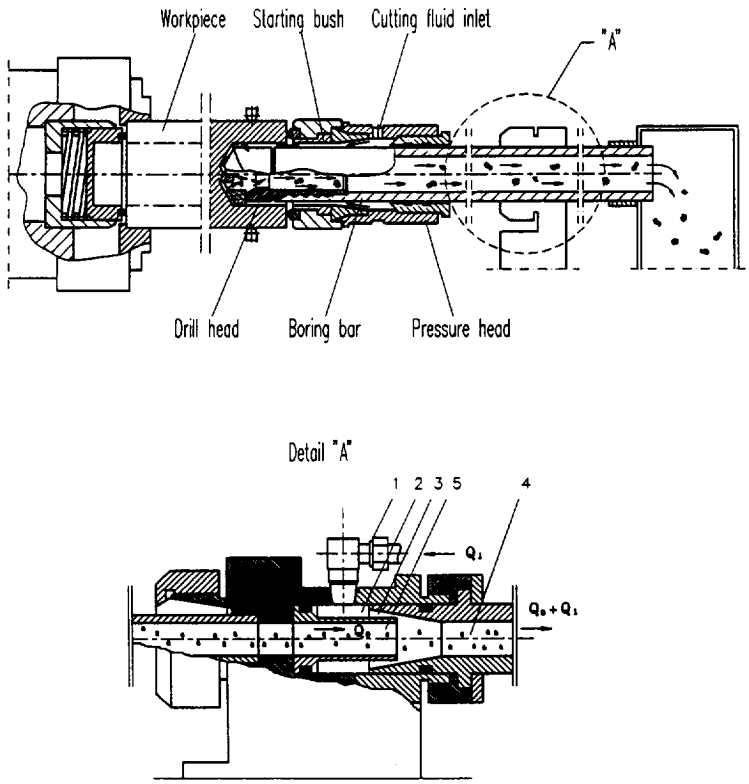

FIG. 15. Introduction of the additional flow rate in B.T.A. drilling using the ejector.

critical velocity. Consequently, the mixture could be transported as far as required by the drilling machine architecture and design. If Q is the cutting fluid–chip mixture flow rate, then the condition for reliable chip transportation is

$$\frac{Q + Q_{\text{add}}}{A_{\max}} \geq v_{\text{cr}}, \tag{24}$$

where $A_{\max}$ is the largest cross-sectional area of the channel in the chip removal system.

5. CONCLUSIONS

The cutting fluid is a very important component of deep hole drilling. The various conditions that exist during the operation and which influence the design of the drill hydraulic system have a great bearing on the efficiency of the drilling operation. These investigations have shown that:

(1) The cutting fluid pressure in the inlet annular channel varies linearly along the length of the channel for both concentric and eccentric walls. The hydraulic resistance of the inlet annular channels with rotating walls increases with an increase in the boring-bar rotational velocity.

(2) The static as well as the dynamic pressure distribution in the machining zone are not uniform. The tests showed that negative pressure exists in the limited space between the bottom of the hole being drilled and the tool flanks (termed "bottom clearance").

(3)The drill head architecture has a significant effect on the pressure distribution in the bottom clearance and, therefore, on tool life and chip removal conditions along the head's chip mouth and chip throat.

(4) Reliable chip removal in BTA and Ejector drilling was achieved under the heterogeneous mode of cutting fluid–chip mixture transportation. The velocity of this

mixture, which corresponds to the beginning of the heterogeneous mode, is known as the critical velocity. A reasonable mixture velocity (and corresponding reasonable flow rate) was recommended to be 15–21% higher than the critical velocity. Reliable chip removing is achieved when this velocity is maintained at any cross-section of the passage in the chip removal system.

Acknowledgements—The financial support of the Natural Science and Engineering Council of Canada as well as the support of the Formation de chercheurs d'action concarte of the Government of Quebec are gratefully acknowledged. Technical support provided by Mr S. Abi Karam, Research Assistant, in data acquisition and drafting is gratefully acknowledged.

REFERENCES

[1] M. O. M. Osman and G. S. Chalil, A theoretical and experimental investigation of coolant flow in gundrilling, *Int. J. Mach. Tool Des. Res.* **19**, 143–155 (1979).
[2] M. O. M. Osman, V. N. Latinovic and B. Greuner, On the performance of cutting fluids for BTA deep-hole machining, *Int. J. Prod. Res.* **19**(5), 491–503 (1981).
[3] V. N. Latinovic and M. O. M. Osman, Friction losses in coolant flow through kidney shape gundrill shank, *Int. J. Prod. Res.* **24**(6), 1319–1329 (1986).
[4] V. P. Astakhov, J. Frazao and M. O. M. Osman, Effective tool geometry for uniform pressure distribution in single edge gundrilling, *Trans. ASME, J. Engng Ind.*, accepted.
[5] V. P. Astakhov and U. N. Suchorucov, The basics of flow conditions in the annular channel of single-side tools (in Russian), *Engng Res. Bull. Irkutsk Polytech. Inst.* 100–106 (1987).
[6] V. P. Astakhov, Modeling of therm-hydraulic processes in the technological systems of the deep-hole machining process (in Russian), *Metallorezushie stanky* **18**, 70–78 (1990).
[7] V. P. Astakhov, The cutting fluid–chip transportation in closed passages of the deep hole machines (in Russian), *Metallorezushie stanky* **17**, 93–97 (1989).